EVALUATION OF IUE HIGH RESOLUTION SPECTRA PROCESSED WITH NEWSIPS

A. Cassatella[1] and R. González-Riestra[2]

[1] Istituto de Astrofisica Spaziale, C.P. 67, I-00044 Frascati (Italy).
[2] Universidad Europea de Madrid, 28670 Villaviciosa de Odón, Madrid, Spain

1 INTRODUCTION

The overall quality of IUE high resolution spectra processed with NEWSIPS is evaluated by studying the accuracy and stability of wavelength determinations, the accuracy of equivalent width determinations, the flux repeatability and the residual camera non-linearities.

The analysis is based on a large number of spectra, mainly of IUE standard stars, obtained with the SWP, LWP and LWR cameras. The spectra were corrected for the echelle blaze function and calibrated in terms of absolute fluxes according to Cassatella et al. (1998). Hereinafter, wavelengths are intended to be in the heliocentric reference frame and in vacuum.

2 Wavelength accuracy

To assess the wavelength accuracy we have considered separately three aspects:

a) the accuracy and repeatability of wavelength measurements of a given spectral feature in several spectra of the same star (see Sect. 2.2);

b) the stability of the wavelength scale along the spectral range covered by each of the cameras (see Sect. 2.3);

c) the consistency of radial velocity determinations obtained from the different cameras.

2.1 Expected accuracy

One of the most important limitations to the wavelength accuracy of IUE high resolution spectra are the target's acquisition errors at the nominal center of the spectrograph's entrance apertures.

From the NEWSIPS dispersion constants and the central wavelengths of spectral orders one can readily deduce that the velocity dispersion corresponding to 1 pixel on the image is practically constant all though the range covered by the cameras, and namely:

$\Delta v = 7.73 \pm 0.05$ km/s for the SWP camera
$\Delta v = 7.26 \pm 0.09$ km/s for the LWP camera
$\Delta v = 7.26 \pm 0.03$ km/s for the LWR camera

To fix our ideas, let us now assume an upper limit of 1 arcsec for the acquisition errors. Taking into account that the plate scale is 1.525 arcsec/pix (Panek 1982), an acquisition error of 1 arcsec would lead to a constant velocity offset v/1.525, i.e. 5.1 km/s for the SWP camera and 4.8 km/s for the long wavelength cameras.

Since the pointing/tracking accuracy is usually better than 1 arcsec, we can consider 5 km/s as an upper limit to the expected wavelength accuracy. Wavelength errors substantially larger than about 5 km/s, might arise internally in the data extraction procedures or can simply be due to spectral noise.

2.2 Repeatability of wavelength determinations

To obtain a reliable information on the self-consistency of wavelength determinations, we have attempted to reduce the effects of spectral noise by performing many measurements of selected narrow and symmetric absorption lines from the interstellar medium, which are strong in some IUE calibration standards, as well as of many emission lines in RR Tel. This study has been carried out separately for the three IUE cameras.

Out of the IUE standards, we have selected BD+28 4211, HD60753, HD93521, BD+75 325, Lambda Lep (HD34816), Zeta Cas (HD 3360) and Eta UMa (HD120315). In addition, we have also used some spectra of the star Zeta Oph (HD149757). Unless otherwise specified, the present measurements all refer to large aperture spectra.

The interstellar lines selected for the SWP range were: SII 1259.520 Å, 1260.421 Å,OI 1302.168 Å and SiII 1304.372 Å. For the LWP and LWR range we have used the K and H components of the MgII doublet at 2796.325 Å and 2803.530 Å and the MgI line at 2852.965 Å. The laboratory wavelengths of the interstellar lines were taken form Morton (1975). The total number of line measurements was 2593, 921 and 519 for the SWP, LWP and LWR cameras, respectively. Examples of line profiles are provided in Fig. 1.

The line positions were initially measured in two ways: a) by fitting a gaussian profile to the observed spectra and b) by computing the line centroid. Since the two methods gave practically the same values, we have at the end adopted method b).

For each target and camera, the radial velocities so obtained were then averaged together. The mean values of the radial velocities, together with the corresponding rms deviation and the number of independent measurements (in brackets) are reported in Table 1. The total number of line measurements was 2593, 921 and 519 for the SWP, LWP and LWR cameras, respectively. Examples of line profiles are provided in Fig. 1.

As it can be deduced from Table 1, the rms repeatability error on radial velocities, averaged over the SWP, LWP and LWR cameras, is 4.2 +/- 1.5 km/s. This value is smaller than

Table 1: *Radial velocities obtained from the SWP, LWP and LWR cameras*

Target	SWP	LWP	LWR
RR Tel	-69.54 ± 6.47 (106) Emission lines	-49.26 ± 3.01 (170) Emission lines	-50.98 ± 4.14 (132) Emission lines
Zeta Oph	-24.65 ± 3.84 (60) SII, SiII		-16.34 ± 3.21 (24) FeII, MnII
Zeta Oph *	-24.7 ± 4.2 (979) SII, SiII, etc	-13.4 ± 2.6 (24) FeII, MnII	-10.2 ± 2.5 (69) FeII, MnII
BD+28 4211	-22.83 ± 6.44 (130) SII, SiII, CII	-5.26 ± 3.60 (40) MgII K	-1.14 ± 4.79 (21) MgII K,H MgI
BD+28 4211 *	-21.6 ± 3.1 (588) SII, SiII, CII	-4.06 ± 3.1 (179) FeII, MgII K, MgI	
HD60753	18.81 ± 6.57 (62) SII, OI, SiII	32.41 ± 6.91 (70) MgII K	29.50 ± 5.81 (24) MgII K,H MgI
HD93521	-38.92 ± 3.97 (68) SII, OI, SiII	-20.73 ± 6.92 (6) MgII K	-19.86 ± 5.36 (18) MgII K,H
BD+75 325	-16.40 ± 4.60 (121) SII, SiII, CII	6.16 ± 2.19 (43) MgI	6.56 ± 3.06 (33) MgII K
BD+75 325 *	-17.2 ± 3.7 (479) SII, SiII, CII	7.4 ± 1.2 (326) FeII, MgII K, MgI	
Lambda Lep		21.18 ± 3.92 (37) MgII K, Mg I	19.25 ± 4.89 (44) MgII K,H
Zeta Cas		-1.09 ± 4.17 (9) MgII K	1.45 ± 4.36 (72) MgII K,H
Eta UMa		-1.12 ± 3.06 (17) MgII K	3.14 ± 7.06 (82) MgII K,H

Notes: 1) The entries for each star are, in the order:
- mean radial velocity, rms (km/s) and number of measurements
- lines used
2) All measurements refer to Large Aperture spectra, except for the
SWP measurements with *, which are an average of LAP and SAP spectra

the upper limit of about 5 km/s expected from acquisition errors. It corresponds to about 1/5 of the spectral resolution (about 21 km/s for any of the cameras; Cassatella and Martin 1982), and is only slightly larger than the velocity dispersion corresponding to half sampling interval (1/2 pix). Considering the presence of spectral noise, we can safely conclude that the repeatability of wavelength (or velocity) determinations provided by NEWSIPS is satisfactory.

A first look to the results in Table 2 indicates that the radial velocities derived from the SWP camera are systematically more negative than those derived from the long wavelength cameras which, on the contrary, give very consistent results. This, and other considerations about the consistency of radial velocity determinations from the three cameras will be discussed in Section 2.4.

2.3 Stability of the wavelength scale along the full spectral range

Table 2: *Mean radial velocities of RR Tel*

a) SWP

Image	Exp. time	Vrad	rms	n
SWP20246	820	-64.0	3.2	25
SWP28741	40	-61.1	2.9	16
SWP29535	220	-73.7	3.0	26
SWP34702	435	-74.2	5.1	28
SWP50717	20	-74.7	2.1	11

b) LWP

Image	Exp. time	Vrad	rms	n
LWP01664	40	-48.2	4.65	27
LWP08728	20	-48.7	4.54	19
LWP08729	40	-43.7	4.90	22
LWP10919	40	-49.4	5.72	28
LWP20538	20	-46.0	6.89	10
LWP23569	20	-46.7	2.11	5
LWP25468	20	-53.8	3.32	6
LWP25953	20	-50.2	7.21	11
LWP25954	95	-48.7	5.02	18
LWP30848	25	-51.4	6.30	14
LWP31348	20	-54.2	7.94	10

b) LWR

Image	Exp. time	Vrad	rms	n
LWR02021	150	-47.3	6.81	48
LWR11744	120	-55.4	5.63	37
LWR16187	540	-50.4	6.35	47

We have studied the accuracy of the wavelength scale over a wide spectral range to look for possible time-dependent distortions across the camera face plate. To this purpose, we have selected 6 SWP,11 LWP and 3 LWR spectra of the emission line object RR Tel obtained at different times. For each spectrum, we have measured the peak wavelengths of several emission lines chosen among those reasonably well exposed and with the cleanest profiles. The highest excitation lines, such as those from [Mg V], were purposely excluded because provided systematically higher negative radial velocities, due to stratification effects within the nebular region. The wavelength range explored is from about 1175 Å to 1860 Å for the SWP camera and 2200 Å to 3100 Å for the long wavelength cameras. A summary of

the measured radial velocities is reported in Table 2.

The mean radial velocities of RR Tel are -69.5 ± 6.5 km/s, -49.26 ± 3.01 km/s, and -50.98 ± 4.1 km/s for the SWP, LWP and LWR cameras, respectively. Since these errors are of the same order of the repeatability errors quoted in Section 2.2, we conclude that the wavelength scales do not present appreciable distortions over the range of wavelengths covered and, within the observational errors, are stable over the period of time considered (1983 to 1994, 1978 to 1983, and 1982 to 1995, for the SWP, LWP and LWR cameras, respectively).

2.4 Consistency of the SWP, LWP and LWR wavelength scales

It clearly appears from Table 1 that there is a close agreement between the radial velocities obtained from the LWP and LWR cameras: we find on average: V(LWP)-V(LWR)= -0.98 ± 2.72 km/s. For this reason, the LWP and LWR radial velocities of the same target were averaged together to obtain a mean value V(LW), using as weights the corresponding number of measurements.

It has been noticed during the present analysis that radial velocities derived from the MgII K and H components of the doublet are consistent, within a couple of km/s in LWR spectra. However, this no longer applies to LWP spectra, where the H component appears systematically 'red' shifted. The velocity difference V(H)-V(K) is on average 9.0 ± 2.4 km/s, if V(H) is determined from order 83 and V(H) from order 82. This peculiarity has not been corrected for, and should be taken into account by users.

Table 1 shows also that there is a non-negligible inconsistency between the velocities derived from the SWP camera and those derived from the LWP and LWR cameras. In Table 3 we report, for each target, the mean radial velocities from SWP spectra, V(SWP) and from long wavelength spectra, V(LW), together with the velocity offset V(SWP) - V(LW). On average, the velocity offset is V(SWP) - V(LW) = 17.7 ± 4.4 km/s.

Table 3 provides also the values of the radial velocities from the literature. For Zeta Oph, we have taken the mean of the following determinations: -14.8 km/s (Barlow et al. 1995; optical), -14.9 km/s (Savage et al. 1992; UV-GHRS), -15.4 ± 4.0 km/s (Brandt et al. 1996; GHRS). The mean value of these measurements is -15.03 km/s. The value for RR Tel is from Thackeray (1977), and the remaining are from the compilation by Duflot, Figon and Meyssonier (1995). The mean difference between the radial velocities form the long wavelength cameras and the literature values is about 5 km/s. The difference is larger and with opposite sign for the SWP camera: about -11 km/s. Given that the primary requirement for the high resolution Final Archive is to provide an internally consistent set of processed data, and considered the uncertainties implied by assuming a single star like Zeta Oph as a velocity standard, the safest approach is to apply a +17.7 km/s correction to the SWP velocity scale. With this correction, large aperture SWP, LWP and LWR spectra should provide a self-consistent radial velocity scale.

A recent investigation has shown that SWP small aperture spectra provide a velocity scale which is consistent, within 1.5 ± 2.6 km/s, with large aperture spectra of the same camera while, on the contrary, small aperture LWR spectra provide radial velocities which are too negative by 13.7 km/s. It has then been decided to apply an additive radial velocity offset of +13.7 km/s to small aperture LWP and LWR spectra.

Table 3: *Mean radial velocities obtained from SWP, LWP and LWR spectra*

V(SWP) km/s	V(LW) km/s	V(LW)-V(SWP) km/s	Target
-69.54	-50.01	19.53	RR Tel
-24.7	-12.12	12.58	Zeta Oph
-21.82	-4.00	17.82	BD+28 4211
18.81	31.67	12.86	HD60753
-38.92	-20.08	18.84	HD93521
-17.04	7.20	24.24	BD+75 325
	20.13		Lambda Lep
	1.17		Zeta Cas
	2.41		Eta UMa

Mean difference V(LW) - V(SWP): 17.65 ± 4.41 km/s

Table 4: *Equivalent widths in SWP spectra of Zeta Oph compared with Morton's (1975) determinations based on Copernicus data*

	Lambda	SWP17335	SWP17936	SWP18163	SWP33330	MORTON
S II	1250.59	0.084	0.089	0.063	0.087	0.100
S II	1253.81	0.098	0.094	0.077	0.101	0.106
S II	1259.52	0.079	0.088	0.085	0.120	0.112
Si II	1260.42	0.163	0.159	0.141	0.204	0.170
C I	1277.24	0.047	0.064	0.057	0.080	0.074
O I	1302.17	0.237	0.208	0.200	0.241	0.201
Si II	1304.37	0.108	0.107	0.110	0.135	0.132
C I	1328.83	0.053	0.041	0.058	0.044	0.052
C II	1334.53	0.181	0.204	0.175	0.211	0.189
C II +	1335.70	0.131	0.156	0.129	0.173	0.140
Si II	1526.71	0.154	0.160	0.180	0.186	0.190
Fe II	1608.46	0.099	0.128	0.132	0.123	0.085
Si II	1808.01	0.065	0.046	0.049	0.054	0.087
Al III	1854.72	0.043	0.051	0.055	0.046	0.057
Al III	1862.79	0.027	0.027	0.030	0.026	0.034

3 Background extraction

It has several times been pointed out that the background extraction for high resolution spectra processed with IUESIPS was not accurate enough especially short ward of about 1400 Å in the SWP camera and 2400 Å in the long wavelength cameras, as denoted by the negative flux numbers assigned to the wings of the strongest emission lines and to the core of the saturated absorption lines. This effect is not present anymore in spectra processed with NEWSIPS, as shown below.

Overestimating or underestimating the background level leads to underestimating or overestimating the fluxes of the emission lines and the equivalent widths of the absorption lines. In the following we report the tests done on the accuracy of the equivalent widths for the SWP, LWP and LWR camera to verify the accuracy of the background extraction.

In addition, as an indirect test of the stability of the background levels, we have used the repeatability of equivalent width determinations.

3.1 SWP

Fig. 2 shows the line profiles of the NV doublet emission and of the broad Lyman alpha feature in the longest exposure available of RR Tel (SWP20246). It is clearly seen that blue and red wings of these lines are not assigned negative values.

Particularly interesting are the NV 'ghost' lines, marked with an asterisk in Fig. 2, which are still present in NEWSIPS data, but sensibly fainter than in data processed with IUESIPS, probably due to the optimized extraction slit. The presence of such spurious features has recently been reported by Zuccolo, Selvelli and Hack (1997) and ascribed to overspilling of the strong NV doublet into adjacent orders.

To verify the accuracy of the background extraction, we have compared the equivalent widths of the strongest interstellar lines in four SWP images of Zeta Oph with those reported by Morton (1975), obtained from Copernicus data. These latter determinations are presumably not affected by background determination problems, unlike IUE echelle spectra near the short wavelength ends of the cameras. The results of the comparison are given in Table 4. A plot of NEWSIPS against Morton's determinations is provided in Fig. 3. The one-to-one correlation between the two sets of data indicates that the measurements form IUE data processed with NEWSIPS are consistent with the ones from Copernicus data. This suggests that the background evaluation for SWP spectra is substantially correct.

3.2 LWP

A first test was based on the ZnII 2026.160 Å line in the LWP 10194 spectrum of SN 1987A, shown in Fig. 4. The ZnII line lies in a region of the LWP camera where the true background is substantially lower than the interorder background; it should therefore provide useful information on the accuracy of the background extraction. Blades et al. (1988) report two components for this line, one due to the galactic foreground at 10 km/s and the other, due to the LMC, at 277 km/s. The ZnII line is in reality blended with MgI 2026.48 Å, providing components at 8 km/s and 282 km/s, which we have not attempted to resolve because are much fainter. The equivalent widths reported by Blades et al. for

the two components of the ZnII-MgI blend, 0.180 Å and 0.315 Å, respectively, should be considered as reliable values because derived from a high signal-to-noise spectrum in the SWP camera which, at these long wavelengths, do not present any particular problem in terms of background extraction. As shown in Table 5, the equivalent widths derived from the LWP and the SWP cameras agree within about 5% on average.

Table 5: *Interstellar lines in SN1987A (LWP 10194)*

Ion	Lambda (lab)	FWHM	EW (present work)	Vrad (present work)	EW (Blades et al.)	Vrad (Blades et al.)
Zn II	2026.160	0.236	0.193	19.5	0.180	10
Zn II	2026.160	0.324	0.324	293.0	0.305	277
Mn II	2576.878	0.261	0.195	24.7	0.220	23
Mn II	2576.878	0.418	0.545	292.5	0.400	289
Mn II	2594.507	0.201	0.158	23.6	0.200	19
Mn II	2594.507	0.277	0.298	292.0	0.355	288

Notes:

The ZnII line is blended with MgI 2026.48 Å. The equivalent widths of the ZnII line include the contribution of the MgI 2026.48 Å line, which is much fainter. On the contrary, the radial velocities refer to the ZnII contribution only.
Velocities (heliocentric) are in km/s.
Wavelengths, FWHM and Equivalent widths (EW) are in A

In the same table we provide, for comparison, the measured equivalent widths of the galactic foreground and the LMC components of the MnII 2576.878 Å, 2594.507 Å interstellar lines, lying in a region of the spectrum which should not be much sensitive to the background extraction, unlike the ZnII line. The comparison was made with the equivalent widths of Blades et al. derived, this time, from a LWP spectrum processed with IUESIPS. The agreement between the two sets of measurements is again quite good except for the high velocity component of the MnII 2594.507 Å line.

The accuracy of the background extraction can also be judged from the cores of strongly saturated absorption lines and from the wings of strongly saturated lines. Fig. 5 shows, for example, two portions of the LWP10919 spectrum of SN1987A, one centered around the FeII lines 2374.46 Å and 2382.76 Å, and the other around the MgII doublet at 2786.35 Å, 2803.53 Å. It appears from the figure that the core of the MgII 2796.35 Å line does not become systematically negative apart from some fluctuations, as expected for a correct background extraction. The situation is slightly worst in the case of the FeII lines, probably due to the higher noise levels in that region. Another example is that of the MgII doublet lines in the longest exposure available of RR Tel (LWP25954), which are strongly saturated. The MgII line profile, plotted in Fig. 6 does not show negative flux values near the line's wings.

Finally, we have measured the equivalent widths of the MgII 2803.53 Å and MgI 2852.97 Å lines in several spectra of BD+28 4211 and BD+75 325. The repeatability error of the MgI equivalent widths is about 7% for BD+28 4211, where this line is quite strong, but it is as large as 36% for BD+75 325, where this line is very faint. As for the MgII line, the repeatability error is about 8% for BD+28 4211 and 14% for BD+75 325.

3.3 LWR

To test of the accuracy of the background extraction for the LWR camera we have measured the equivalent widths of 6 strong FeII and MnII interstellar lines in 4 LWR spectra of the star Zeta Oph, and compared them with measurements based on Copernicus data. The line used are FeII 2344.213 Å, 2382.760 Å, 2586.650 Å and 2600.172 Å, and MnII 2576.878 Å and 2606.476 Å. A plot of the region 2570 Å to 2610 Å, from LWR11291 is shown in Fig. 7.

The LWR equivalent width measurements are reported in Table 6 together with the corresponding values from the Copernicus experiment, as provided by Morton (1975). A plot of the present measurements versus Morton's values is given in Fig. 8. As one can appreciate from the figure, there is a good agreement between the two sets of equivalent widths, and no systematic departures are seen.

A further test of the background determination was done by measuring the ZnII 2026.160 Å line in 4 spectra of Zeta Oph (see Fig. 7). At these short wavelengths the true background, and then the equivalent widths, are quite difficult to determine accurately. Still, the four determinations of the ZnII equivalent width, with a mean value of 0.111 +/- 0.032 Å, are in a reasonable agreement with Morton's value of 0.095 Å, considered as uncertain by this author. The ZnII data points are overplotted as crosses in Fig. 8.

The accuracy of the background extraction can also be judged from the cores of strongly saturated absorption lines and from the wings of strongly saturated emission lines. Fig. 9 shows, for example, the [MgV] 2782.8 Å and the MgII doublet lines in the longest exposure available of RR Tel (LWR16187), which are strongly saturated. As shown in the figure, the flux near the line wings does not reach negative values except for the 2803.53 Å component of MgII. We ascribe these negative values as due to the noise level near the short wavelength end of order 82. Another example is given in Fig. 10, showing a LWR spectrum of Eta Car centered around the MgII doublet at 2786.35 Å, 2803.53 Å. It appears from the figure that the flux level in the core of the MgII lines is substantially correct except for the 2803.53 A component, whose core goes slightly below the zero level.

Finally, we have measured the equivalent widths of the MgII 2796.352 Å and 2803.53 Å lines in 41 spectra of Eta Uma, 36 spectra of Zeta Cas and 22 spectra of Lambda Lep. The repeatability error of the MgII ranges from 11 to 30% in the case of Eta Uma, where these lines are faint, but is considerably better, about 5.3% in Zeta Cas and Lambda Lep, where these lines are strong and little disturbed by noise. The stability of equivalent width determinations for strong interstellar lines is then very similar to that of the SWP and LWP cameras.

Table 6: *LWR Measurements (Equivalent Widths, FWHM and Radial Velocities in Zeta Ophiuchi*

LWR 11728				MORTON		
LAMBDA	E.W.	FWHM	Vrad	Vrad	E.W.	Ion
2382.760	0.227	0.380	-21.748	-15.34	0.238	FeII (2)
2576.878	0.209	0.240	-22.436	-12.45	0.138	MnII (1)
2586.650	0.172	0.270	-21.816	-12.86	0.214	FeII (1)
2594.507	0.110	0.250	-14.951	-12.82	0.116	MnII (1)
2600.172	0.228	0.300	-16.045	-12.22	0.226	FeII (1)
2606.476	0.095	0.290	-14.462	-10.35	0.111	MnII (1)

LWR 11290				MORTON		
LAMBDA	E.W.	FWHM	Vrad	Vrad	E.W.	Ion
2382.760	0.214	0.260	-14.161	-15.34	0.238	FeII (2)
2576.878	0.127	0.280	-15.338	-12.45	0.138	MnII (1)
2586.650	0.191	0.290	-18.223	-12.86	0.214	FeII (1)
2594.507	0.127	0.240	-11.961	-12.82	0.116	MnII (1)
2600.172	0.233	0.280	-11.766	-12.22	0.226	FeII (1)
2606.476	0.087	0.260	-14.265	-10.35	0.111	MnII (1)

LWR 11291				MORTON		
LAMBDA	E.W.	FWHM	Vrad	Vrad	E.W.	Ion
2382.760	0.223	0.280	-15.021	-15.34	0.238	FeII (2)
2576.878	0.094	0.250	-18.576	-12.45	0.138	MnII (1)
2586.650	0.199	0.290	-19.496	-12.86	0.214	FeII (1)
2594.507	0.117	0.210	-12.497	-12.82	0.116	MnII (1)
2600.172	0.237	0.290	-14.384	-12.22	0.226	FeII (1)
2606.476	0.069	0.290	-15.753	-10.35	0.111	MnII (1)

LWR 11292				MORTON		
LAMBDA	E.W.	FWHM	Vrad	Vrad	E.W.	Ion
2382.760	0.232	0.280	-16.741	-15.34	0.238	FeII (2)
2576.878	0.127	0.260	-18.917	-12.45	0.138	MnII (1)
2586.650	0.200	0.310	-21.080	-12.86	0.214	FeII (1)
2594.507	0.123	0.250	-13.654	-12.82	0.116	MnII (1)
2600.172	0.243	0.290	-13.568	-12.22	0.226	FeII (1)
2606.476	0.097	0.260	-15.388	-10.35	0.111	MnII (1)
Mean			-16.34	-12.67		
rms			3.21	1.49		

4 Flux repeatability

4.1 SWP

We have performed a test of the flux repeatability using 45 high resolution spectra of HD93521 (12 spectra), BD+28 4211 (two groups of 5 and 7 spectra each), HD60753 (two groups of 5 and 8 spectra each) and BD+75 325 (8 spectra). The spectra in each group were obtained close enough in time to minimize the effects of camera sensitivity degradation.

The test was done in 6 wavelength bands 5 A wide spanning the wavelength interval from 1185 to 1790 Å. In Table 7 we report, for each group of spectra, the percent rms deviation from the mean ripple-corrected net flux in the band, which we take as a measure of the flux repeatability. Table 8 shows that the repeatability for spectra obtained sufficiently close in time is about 2%. A similar repeatability test made on a larger amount of spectra needing correction for the camera time-dependent sensitivity degradation provides repeatability errors ranging from 3% to 4% Cassatella et al. (1998). These larger repeatability errors are most likely due to the intrinsic uncertainties in the sensitivity degradation algorithm.

4.2 LWP

We have tested the flux repeatability using a total of 28 optimum exposure of BD+75 325. The spectra were divided in three groups each containing images obtained in a restricted period of time. In this way we have avoided to correct for the time-dependent sensitivity degradation of the camera.

The flux repeatability was evaluated, for each group, in 4 wavelength bands 5 A wide centered at 2120 Å, 2460 Å, 2925 Å and 3120 Å, corresponding to the central parts of orders 109, 94, 79 and 74, respectively. The flux repeatability was measured as the percent rms deviation from the mean flux in the band. The results of the measurements, performed on the ripple corrected net spectra, are reported in Table 8.

As one can appreciate from Table 8, the repeatability errors can reach the 4%-5% level near the short and long wavelength end of the cameras, but are about a factor of two lower in the 2460 Å and 2925 Å bands. A similar repeatability test done on a larger amount of spectra needing correction for the camera time-dependent sensitivity degradation provides errors of about the same amount (Cassatella et al. 1998). This result confirms that the sensitivity degradation algorithm adopted for the LWP camera is essentially correct.

4.3 LWR

We have tested the flux repeatability using a total of 11 optimum exposure of Eta Uma and 9 of Zeta Cas. The spectra were divided in four groups each containing images obtained in a restricted period of time. In this way we have avoided to correct for the time-dependent sensitivity degradation of the camera.

The flux repeatability was evaluated, for each group, in 4 wavelength bands 5 A wide centered at 2122 Å, 2459 Å, 2926 Å and 3080 Å, corresponding to the central parts of orders 109, 94, 79 and 75, respectively. The flux repeatability was measured as the percent rms deviation from the mean flux in the band. The results of the measurements, performed on the ripple corrected net spectra, are reported in Table 9.

Table 7: *Repeatability test for high resolution SWP spectra*

Band	% rms deviation	order #
1185 - 1190	3.2	116
1225 - 1230	2.3	112
1285 - 1290	2.6	107
1375 - 1380	1.8	100
1485 - 1490	1.6	93
1595 - 1600	3.5	86
1795 - 1800	1.6	77

SWP images used:

NGC 246:
41997, 42104, 42214, 42247, 47843, 47844

HD60753:
a) 8704, 8705, 9093, 9094, 9095
b) 29842, 30431, 32886, 33025, 34175,
35509, 35579, 36298

BD+75 325:
35153, 35351, 35405, 35459, 35710, 35881,
36179, 36180

HD93521:
30621, 30622, 30623, 30624, 30625, 30626,
30627, 30628, 30629, 30630, 30631

BD+28 4211:
a) 28519, 28607, 29914, 29869, 29925
b) 40209, 40219, 40440, 40441, 41996, 42103,
46202

As one can appreciate from Table 9, the repeatability errors reach 4% near the short wavelength end of the camera, decrease to about 1.8% in the region of maximum sensitivity and increase again to 2.3% near the long wavelength end of the camera.

5 Linearity

5.1 SWP

There are just a few high resolution data which are suitable for testing the SWP linearity. The most complete set consists of 7 images of CD-38 10980 obtained in 1991, with exposure times ranging from about 50% to 180% of the optimum exposure time (200 min). For these

Table 8: *LWP repeatability test using high resolution spectra of BD+75 325*

ORDER	WAVELENGTH	MEAN FN/t	r.m.s.	Repeatability	Group
109	2120	0.09950	0.00516	5.18 %	A
		0.09800	0.00508	5.18 %	B
		0.09359	0.00413	4.41 %	C
94	2460	0.18288	0.00379	2.07 %	A
		0.17288	0.00322	1.86 %	B
		0.16490	0.00335	2.03 %	C
79	2925	0.18244	0.00313	1.71 %	A
		0.17533	0.00296	1.69 %	B
		0.16850	0.00330	1.95 %	C
74	3120	0.05281	0.00239	4.53 %	A
		0.04932	0.00096	1.94 %	B
		0.04884	0.00128	2.62 %	C

Notes: 1) The bands are 6 Å wide centered at the wavelengths in Col. 2
2) The groups in Col. 6 refer to the following LWP images:
Group A: 5611, 6812, 6728, 6832, 6789, 6822, 6826, 6959, 7374, 7410, 9724 (March to December 1985)
Group B: 14836, 14942, 14918, 15151, 15129, 15130, 16483, 16491, 16984 (January to December 1989)
Group C: 22343, 22345, 22378, 22725, 23871, 23987, 24158, 24631 (February to November 1992)

images we have measured the mean flux in 5 bands 5 Å wide starting at 1185, 1285, 1485, 1595 and 1785 Å. We have averaged the flux in each band and divided it by the mean flux of the two 100% exposures (SWP41466 and SWP42260). The ratios so obtained, given in Table 10, indicate departures from linearity ranging from -6% at 1185 Å to +4% at 1785 Å for the 49.5% exposure and up to -5 % in the 69.5% exposure.

The second set consists of 5 images of BD+28 321 obtained between June and August 1979, with exposure times 37.5%, 62%, 85%, 100% and 150% of the optimum exposure time. The maximum departure from linearity in this set ranges form -2% to 5% for the 150% and the 37.5% exposures, respectively.

5.2 LWP

The LWP high resolution linearity test was performed using 17 spectra of the calibration standards BD+28 4211 and BD+75 325 covering the range of exposure levels from 27% to 207% of the optimum exposure time. The test was performed in 4 wavelength bands centered at 2120, 2460, 2925 and 3132 Å. The total band width was 6 Å. These bands were selected for being relatively free from strong absorption lines.

The results of the test are given in Table 11 which provides, for each band, the ratio

Table 9: *Repeatability test for LWR high resolution spectra*

Band	Order	% rms	group
2122 A	109	4.92	a
		5.64	b
		3.76	c
		2.43	d
2459 A	94	3.80	a
		3.68	b
		2.72	c
		3.30	d
2926 A	79	1.52	a
		2.55	b
		1.80	c
		1.42	d
3080 A	75	2.90	a
		2.85	b
		1.93	c
		1.72	d

group a) Zeta Cas:
LWR12211,LWR14110,LWR14717,LWR14820
(DEC. 1981 - DEC. 1982)
group b) Zeta Cas
LWR16760,LWR17004,LWR17201,LWR17473,LWR17474
(SEPT. 1983 - JUL. 1984)
group c) Eta UMa
LWR10102,LWR11582,LWR11948,LWR12319,LWR12807,LWR12978
(MAR. 1981 - APR. 1982)
group d) Eta UMa
LWR13856,LWR14540,LWR14889,LWR15628,LWR16267)
(AUG. 1982 - JUN. 1986)

between the mean flux corresponding to a given exposure level and the mean flux of the 100% exposures.

As shown in the table, the maximum departures from linearity, reaching 8% are found for the 133% level at 2120 Å and for the 207% level near the regions of maximum sensitivity of the camera. The latter deviations can be easily understood in terms of camera saturation. In any case, the linearity properties deduced from the LWP high resolution spectra appear to be better than those derived from LWP low resolution data (González-Riestra 1998).

Table 10: *Linearity test for SWP high resolution spectra*

Table 10: Linearity test for SWP high resolution spectra

IMAGE	t(min)	t/t(opt)	1185 A	1285 A	1485 A	1595 A	1785 A
41467	99	0.495	0.9370	0.9480	0.9730	1.0350	1.0480
41346	135	0.675	0.9220	0.9750	0.9490	1.0270	1.0230
42309	139	0.695	0.9670	0.9340	0.9790	0.9920	1.0020
41435	180	0.900	0.9580	0.9870	1.0070	0.9650	0.9940
41466	200	1.000	0.9810	0.9820	0.9950	0.9950	0.9750
42260	200	1.000	1.0190	1.0180	1.0050	1.0050	1.0250
41495	360	1.800	0.9550	0.9830	0.9780	0.9610	0.9920

Note: Col. 4 to 8 report the flux ratios of a given image with
respect to the 100% exposures SWP 41466 and SWP42260

Table 11: *Linearity test for LWP high resolution spectra*

LEVEL	2120 A	2460 A	2925 A	3132 A	Group
27%	1.031	1.026	0.983	0.976	A
41%	1.004	1.017	0.994	0.983	B
67%	0.988	1.024	1.030	1.000	C
83%	0.946	0.982	0.997	0.968	D
100%	1.000	1.000	1.000	1.000	E
133%	0.929	1.030	1.003	1.026	F
207%	1.008	1.041	1.038	1.079	G

Notes: 1) The bands are 6 A wide
2) The groups in Col. 6 refer to the following LWP images:
Group A: 18021, 18121 (BD+28 4211)
Group B: 14961 (BD+28 4211)
Group C: 19302, 19291 (BD+28 4211)
Group D: 17321, 17394 (BD+75 325)
Group E: 17526, 17547, 17570, 19431 (BD+75 325)
17977, 18880, 19290, 19460 (BD+28 4211)
Group F: 17327 (BD+75 325)
Group G: 17328 (BD+75 325)

5.3 LWR

For the LWR high resolution linearity test we only dispose of 5 images obtained in the period July 1980 to February 1981, covering the range of exposure times from 50% to 250% of the optimum exposure time. The test was performed in 4 wavelength bands 6 Å wide centered at 2122, 2459, 2926 and 3080 Å (i.e. near the center of orders 109, 94, 79 and 75, respectively). These bands were selected for being relatively free from strong absorption lines.

The results of the test are provided in Table 12 which gives, for each band, the ratio between the mean flux corresponding to a given exposure level and the mean flux of the 100% exposures.

As shown in the table, the maximum departures from linearity, reaching 25% are found at the shortest wavelengths, where fluxes are underestimated by 25% for the 50% exposure, and overestimated by 12% for the 250% exposure.

Table 12: *Linearity test for LWR high resolution spectra*

LEVEL	2122 A	2459 A	2926 A	3080 A	GROUP
50%	0.75	0.98	0.99	0.91	A
100%	1.00	1.00	1.00	1.00	B
225%	1.18	1.05	1.00	1.01	C
250%	1.12	1.04	1.01	1.00	D

GROUPS.

A) LWR09995 (HD90753)
B) LWR09954 (HD90753)
D) LWR09114, LWR09113 (HD90753)
E) LWR 8116 (HD90753)

6 CONCLUSIONS

The internal accuracy on wavelength determinations provided by IUE high resolution spectra processed with NEWSIPS is 4.2 +/- 1.5 km/s, irrespective of the camera used. This value is smaller than the upper limit of about 5 km/s expected from acquisition errors. It corresponds to about 1/5 of the spectral resolution (about 21 km/s for any of the cameras; Cassatella and Martín 1982), and is only slightly larger that the velocity dispersion corresponding to half sampling interval (1/2 pix). Considering the presence of

spectral noise, we can safely conclude that the repeatability of wavelength (or velocity) determinations provided by NEWSIPS is satisfactory.

Radial velocity measurements of the emission lines in RR Tel in the SWP, LWP and LWR cameras obtained over a wide span of time do not reveal distortions of the wavelength scale larger than the limit set by the internal uncertainty of the measurements.

It has been found also that radial velocities derived from large aperture SWP spectra are systematically more negative than those derived from large aperture LWP and LWR spectra (these two latter are consistent with each other). The velocity offset V(SWP) - V(LW) is -17.7 km/s.

SWP small aperture spectra provide a velocity scale which is consistent, within 1.5 +/- 2.6 km/s, with large aperture spectra of the same camera while, on the contrary, small aperture LWR spectra provide radial velocities which are too negative by 13.7 km/s.

INES spectra will then incorporate an additive radial velocity correction of +13.7 km/s to small aperture LWP and LWR spectra and of +17.7 km/s to SWP large and small aperture spectra. No correction will be applied to large aperture LWP and LWR spectra.

For the SWP and LWR cameras, we have tested the accuracy of the background extraction by comparing the equivalent widths of strong interstellar lines with similar measurements obtained through the Copernicus experiment, presumably not affected by problems in the background evaluation. The close agreement between the two sets of data suggest that the NEWSIPS background extraction is substantially correct. Irrespective of the camera used, we have found that the wings of the strong emission lines and the cores of the strong absorption lines do not reach negative values, like seen in spectra processed with IUESIPS, especially at the shortest wavelengths. This fact, together with the satisfactory repeatability performance of equivalent widths from many spectra obtained under different observing conditions suggests that the background extraction algorithm is sufficiently stable and accurate.

In terms of flux repeatability, we find that absolute fluxes obtained from SWP, LWP and LWR high resolution spectra obtained close in time are repeatable within about 2% to 4 % near the regions of maximum sensitivity.

We have tested the linearity properties of high resolution spectra in the range of exposure levels 37.5% to 150% for the SWP camera, 27% to 207% for the LWP camera and 50% to 250% for the LWR camera. The results indicate that there are moderate departures from linearity especially for sensibly underexposed spectra and near the short and long wavelength edges of the cameras. Similar effects have been noticed in IUE low resolution spectra (González-Riestra 1998).

Acknowledgements

We are thankful to N. Loiseau for the improvements done to this document.

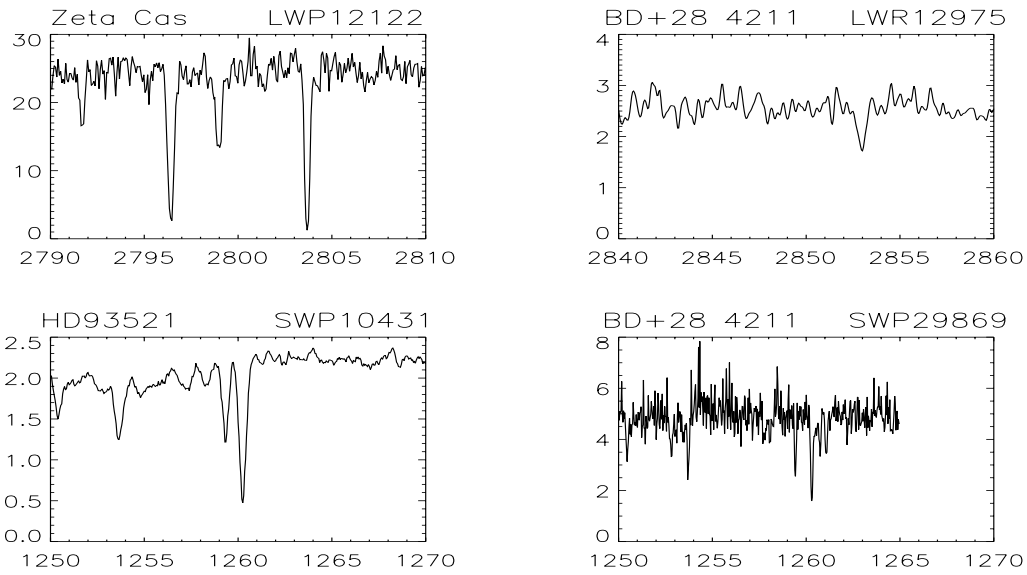

Figure 1: *Typical profiles of the interstellar lines in some of the IUE standards: The Mg II doublet in Zeta Cas (LWP12112); the MgI 2852.956 Å line in BD+28 4211; the SII 1259.52 Å and SiII 1260.421 Å lines in HD93521 and BD+28 4211.*

References

[1] Barlow M.J., Crawford J.A., Diego F. et al.: 1995, MNRAS 272, 333.

[2] Blades J.C., Wheatley J.M., Panagia N. et al.: 1988, Ap.J. 334, 308.

[3] Brandt J.C. et al: 1996, AJ 112, 1128.

[4] Cassatella A., Martín, T. 1982, Proceedings of the Three-Agency Meeting, ESA.

[5] Cassatella A. et al., 1998, in preparation.

[6] Duflot M., Figon P., Meyssonier N.: 1995, A&A Suppl. 114, 269.

[7] González-Riestra R.: 1998, in 'Ultraviolet Astronomy beyond the IUE Final Archive', Sevilla, Nov. 1997, in press.

[8] Morton D.C., 1975, ApJ 197, 85.

[9] Panek R.J.,1982, Proceedings of the Three Agency Meeting, ESA.

[10] Thackeray A.D.: 1977, MNRAS 83, 1

[11] Zuccolo R., Selvelli P.L., Hack M., 1997, A&A, in press.

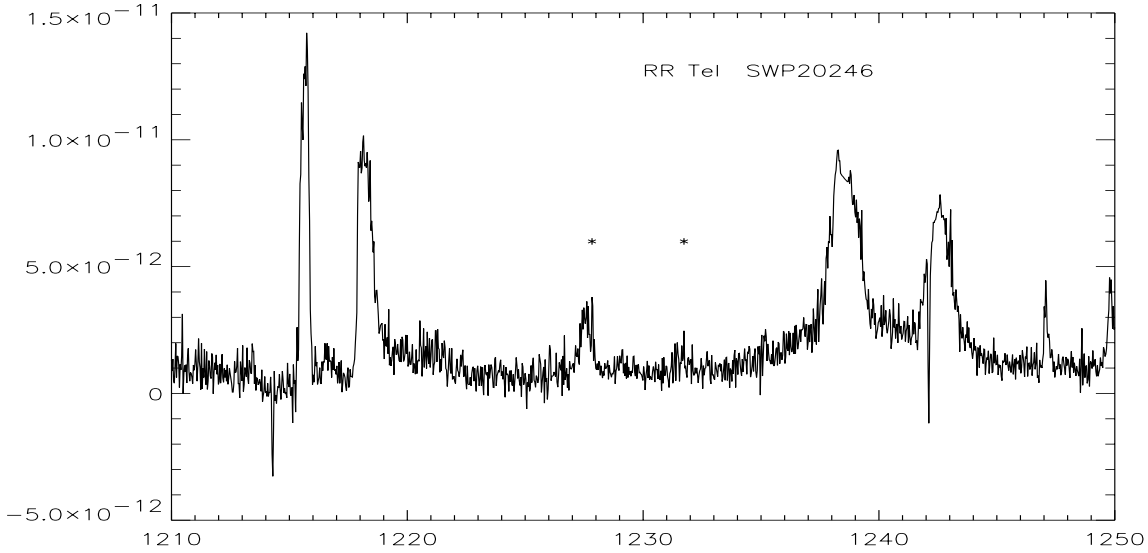

Figure 2: *The Ly_α and NV emissions in the longest exposure available of RR Tel (SWP20246, 820 min). The Ly_α emissions are from the geocorona (in the large and small aperture). The two features labeled with an asterisk are due overspilling of the strong NV emission into the adjacent order.*

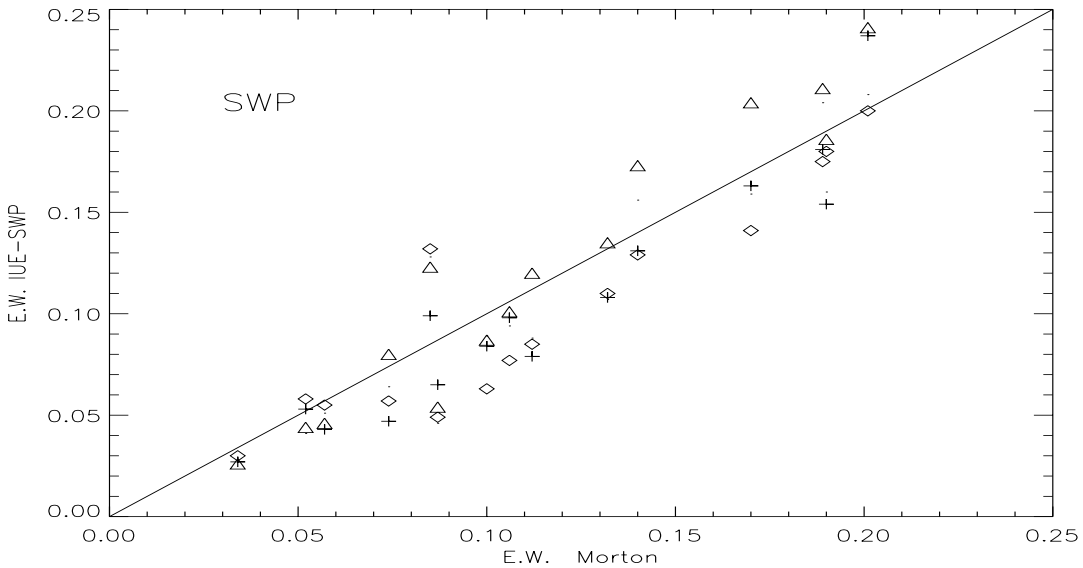

Figure 3: *Comparison between equivalent widths determinations from Copernicus data (Morton 1975) and from IUE data processed with NEWSIPS.*

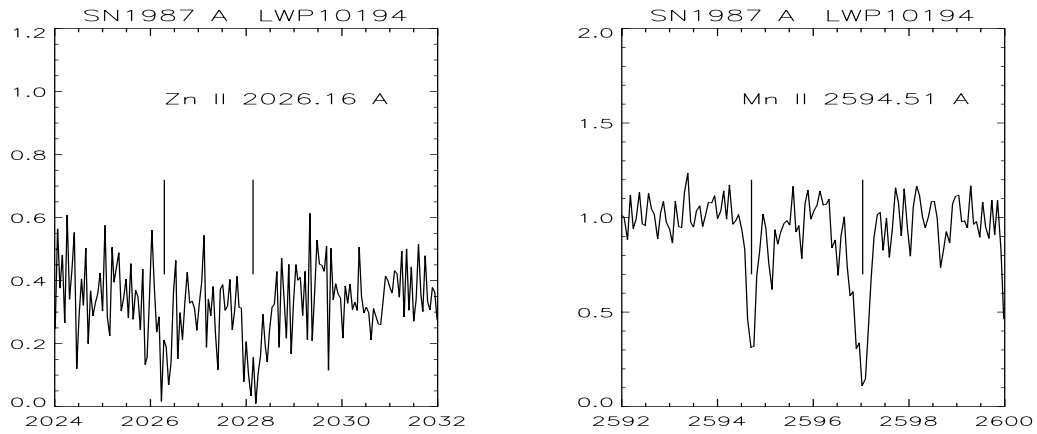

Figure 4: *Profiles of the interstellar lines of ZnII and MnII in a LWP spectrum of SN 1987A. The equivalent widths of the ZnII components (galactic foreground and LMC) were used to test the accuracy of the background extraction through a comparison with determinations made in the SWP range by Blades et al. (1988).*

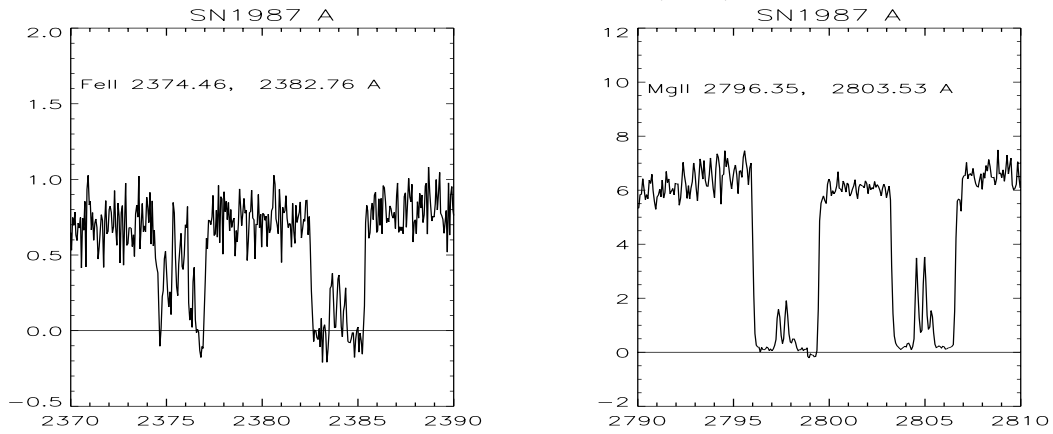

Figure 5: *Line profiles of a blend of two FeII lines and of the MgII doublet in SN 1987A. The saturated core of these lines was used to test the background extraction.*

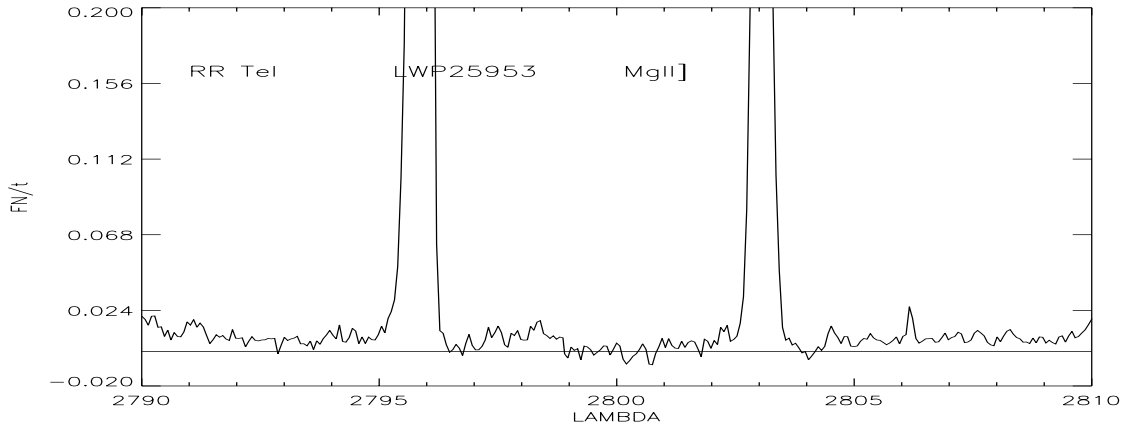

Figure 6: *The MgII doublet in a long exposure of RR Tel (LWP25953).*

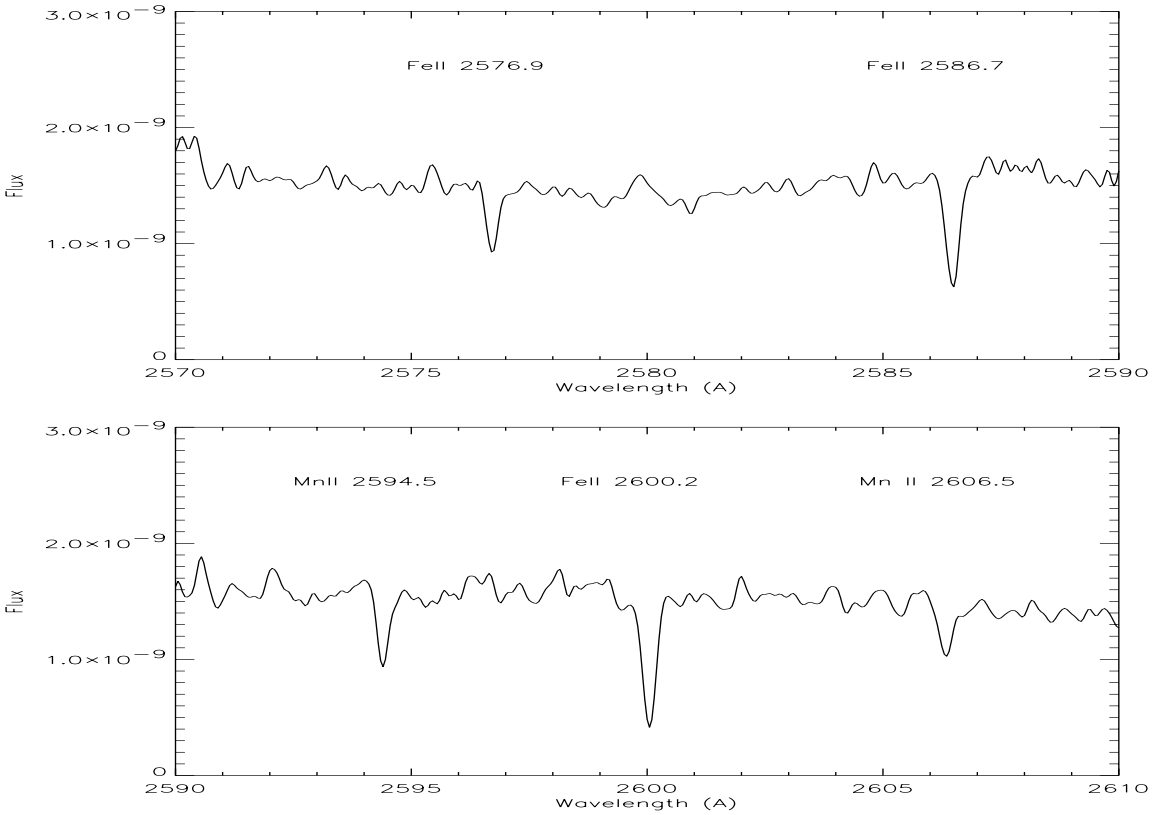

Figure 7: *Profiles of the interstellar lines of FeII and MnII in a LWR spectrum of Zeta Oph. These lines were used to test the wavelength accuracy of LWR spectra against Morton's (1975) determinations based on Copernicus data.*

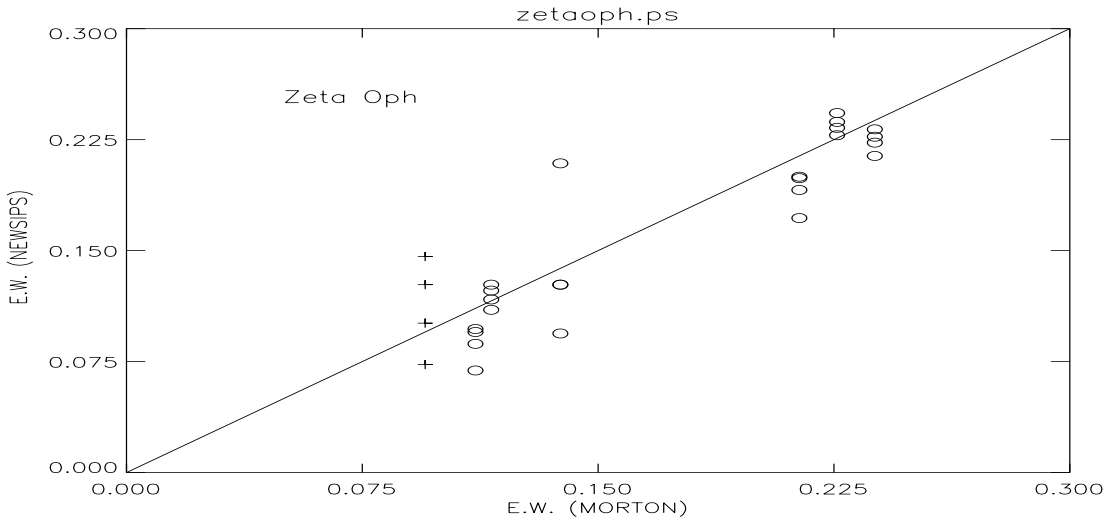

Figure 8: *The equivalent widths of the interstellar lines in Zeta Oph as measured in 4 LWR spectra are plotted against Morton's (1975) determinations based on Copernicus data. The crosses correspond to the ZnII line at 2026 Å.*

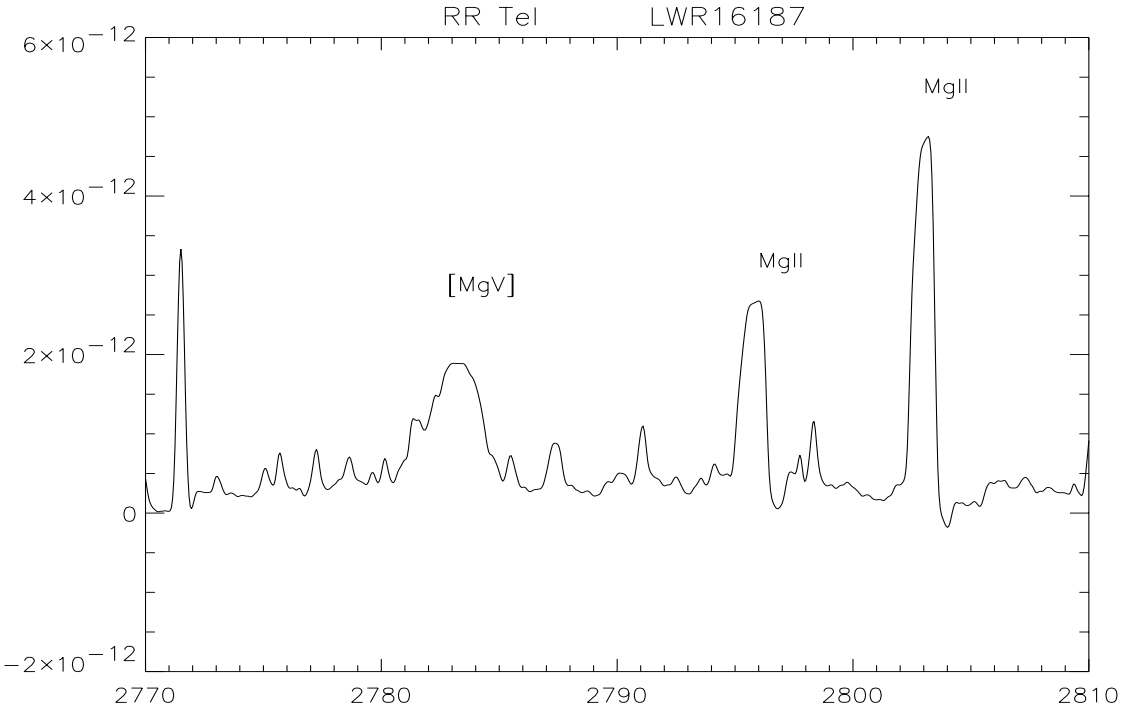

Figure 9: *Spectral region showing the profiles of the MgII doublet and of the [MgV] 2782.8 A broad line in RR Tel.*

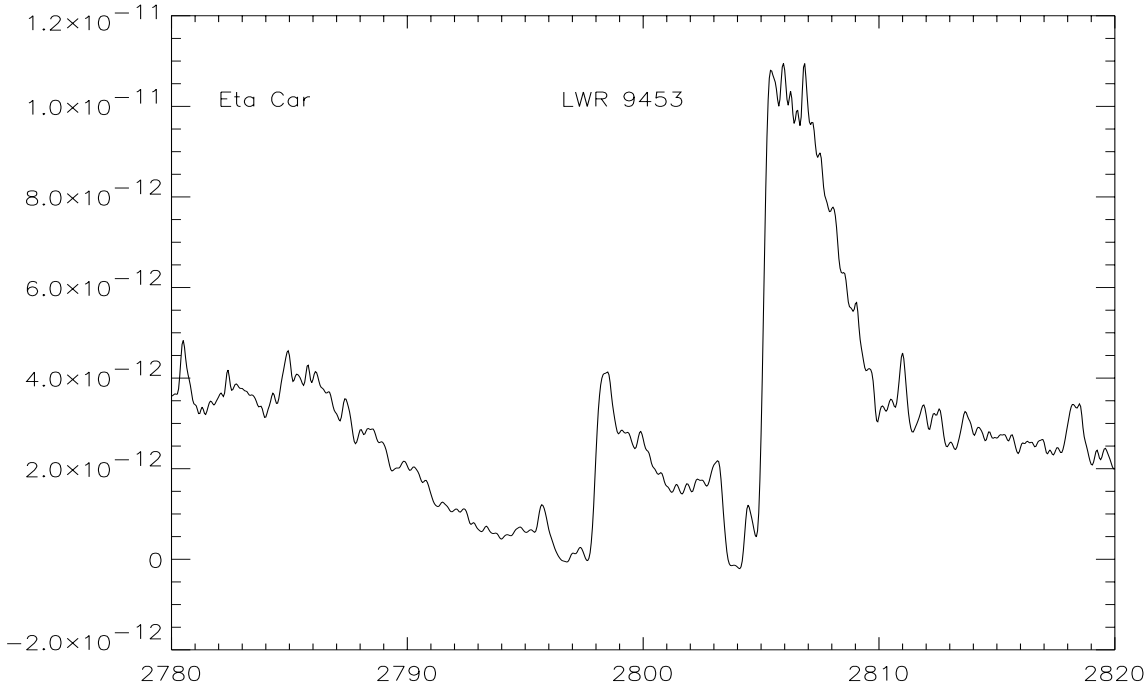

Figure 10: *Profile of the MgII doublet in Eta Car (LWR9453).*